European Radiology (2019) 29:3170–3182
https://doi.org/10.1007/s00330-018-5903-3

ONCOLOGY

Alveolar soft-part sarcoma: can MRI help discriminating from other soft-tissue tumors? A study of the French sarcoma group

Amandine Crombé[1,2] · Hervé J. Brisse[3,4] · Pauline Ledoux[1] · Leila Haddag-Miliani[5] · Amine Bouhamama[6] · Sophie Taieb[7] · François Le Loarer[2,8] · Michèle Kind[1]

Received: 19 September 2018 / Revised: 25 October 2018 / Accepted: 22 November 2018 / Published online: 17 December 2018

Abstract

Objectives To investigate the imaging features of alveolar soft-part sarcomas (ASPS) on pre-treatment MRI in order to identify relevant criteria to distinguish ASPS from other soft-tissue tumors.

Methods A series of 25 patients (mean age, 18.5 years old) with histologically proven ASPS from five French comprehensive cancer centers was compared to a control cohort of 292 patients with various histologically proven benign and malignant soft-tissue tumors representative of the 10-year long activity of one center. All had a baseline MRI with contrast-agent administration. Two radiologists independently reviewed the MRIs. Features assessing location, size, signal, architecture, periphery, and vascularization were reported. Their association with the histological diagnosis of ASPS was evaluated with chi-square or Fisher's test. Their prevalence, sensitivity, specificity, odds ratio, and reproducibility were calculated.

Results Eight MRI features were significantly associated with ASPS: deep location ($p < 0.001$), high signal intensities on T1-weighted imaging ($p < 0.001$), central area of necrosis ($p = 0.001$), absence of fibrotic component ($p = 0.003$), infiltrative growth pattern ($p = 0.003$), absence of tail sign ($p = 0.001$), presence of intra- and peritumoral flow-voids ($p < 0.001$), and number of flow-voids ≥ 5 ($p < 0.001$). Twenty out of the 25 (80%) ASPS showed at least 7 of these 8 features compared to only four out of 292 (1.4%) tumors of the control cohort (1 benign vascular tumor, 1 solitary fibrous tumor, 2 high-grade soft-tissue sarcomas). The five ASPS with less than 7 out of 8 features measured less than 40 mm.

Conclusion The striking histological uniformity of ASPS translates into imaging. However, ASPS may be misdiagnosed as benign tumors or pseudo-tumors, notably intramuscular benign vascular tumors or vascular malformations.

Key Points

- *ASPS are rare aggressive mesenchymal tumors displaying recurrent MRI features highly reminiscent of the diagnosis.*
- *Deep-seated tumors presenting with mainly high signal intensity on T1-weighted imaging, an absence of fibrotic component, ill-defined margins without aponeurotic extension, and more than five central and peripheral flow-voids are very likely to be ASPS.*
- *ASPS may be misdiagnosed as intramuscular benign vascular tumor or vascular malformation, which occur in the same age group.*

Keywords Magnetic resonance imaging · Neoplasms, connective and soft tissue · Sarcoma · Sarcoma, alveolar soft part · Hemangioma, intramuscular

Electronic supplementary material The online version of this article (https://doi.org/10.1007/s00330-018-5903-3) contains supplementary material, which is available to authorized users.

✉ Amandine Crombé
a.crombe@bordeaux.unicancer.fr

[1] Department of Radiology, Institut Bergonié, Regional Comprehensive Cancer Center, 229 cours de l'Argonne, F-33076 Bordeaux, France

[2] University of Bordeaux, F-33000 Bordeaux, France

[3] Imaging Department, Institut Curie, 75005 Paris, France

[4] Paris Sciences et Lettres Research University, Paris, France

[5] Department of Radiology, Institut Gustave Roussy, Comprehensive Cancer Center, 94800 Villejuif, France

[6] Department of Radiology, Centre Léon Bérard, Comprehensive Cancer Center, 69008 Lyon, France

[7] Department of Radiology, Centre Oscar Lambret, Comprehensive Cancer Center, 59000 Lille, France

[8] Department of Pathology, Institut Bergonié, Comprehensive Cancer Center, 33076 Bordeaux, France

Abbreviations

ASPS	Alveolar soft-part sarcoma
CI95%	95% confidence interval
FNCLCC	French Federation of Cancer Centers Sarcoma Group
ICC	Interclass correlation coefficient
ISSVA	International Society for the Study of Vascular Anomalies
OR	Odds ratio
PACS	Picture archiving and communication system
SFT	Solitary fibrous tumor
STS	Soft-tissue sarcoma
WI	Weighted imaging
κ	Cohen's kappa
κw	Weighted kappa

Introduction

Alveolar soft-part sarcoma (ASPS) is a rare mesenchymal tumor that represents 0.4–1% of all soft-tissue sarcomas (STS) [1]. ASPS mostly occurs in young adults, and about one third of cases affect children and adolescents [2]. It was first described in 1952 by Christopherson who noticed the striking uniformity from one area of the tumor to another and from one tumor to another [3]. Indeed, ASPS demonstrates a pseudoalveolar pattern made of uniform and repeated nests of large granular cells delineated by fibrous septa containing vascular channels [1]. Thereafter, cytogenetical analyses identified a recurrent translocation responsible for the formation of a chimeric transcription factor (ASPL-TFE3) leading to the upregulation of pro-angiogenic transcripts [4]. These pseudoalveolar patterns and pronounced angiogenesis translate into imaging, especially MRI, through a lobular architecture, high signal intensities (SI) on T1-weighted imaging (-WI), which may be due to the abundance of capillary vascularization and blood stagnation within sinusoidal vascular channels and large feeding vessels and flow-voids [5–13].

ASPS can remain clinically indolent for a long-time although half of the patients have metastatic diseases at diagnosis. Distant metastases mainly occur in the lung, but locations in the bone, brain, and liver are observed as well [14, 15]. This high propensity for hematogenous metastases has been related to their abundant neovascularization and to their ability to form intravascular endothelial-wrapped clusters of tumor cells released in the circulation [1, 16, 17].

Radiological literature on ASPS is relatively scarce, including small series and reports of patients, some being misdiagnosed as hemangioma or arterio-venous malformations [5, 13]. In addition, solitary fibrous tumors, desmoid tumors, schwannoma, or certain STS can also present with imaging features linked to ASPS, especially abnormal intra- and peritumoral vascularity [18–22]. Therefore, the aims of this study were to investigate the imaging features on pre-treatment MRI that could help to distinguish ASPS from other soft-tissue masses and to find clues to avoid misdiagnosis especially with benign tumors that may not be systematically biopsied.

Materials and methods

Study design

This retrospective case-control study was approved by the institutional review board, and informed consent was waived. The population study was made of two cohorts: ASPS patients (cases) and patients with non-ASPS soft-tissue masses (control cohort).

Patients with ASPS were retrieved through the CONTICABASE (Connective Tissue in Cancer Network), a European sarcoma database and tumor bank comprising a second opinion of an expert sarcoma pathologist from 1997 to 2018 [23]. Due to the rarity of ASPS, patients came from five French comprehensive cancer centers: Institut Curie, Institut Gustave Roussy, Centre Léon Bérard, Centre Oscar Lambret, and Institut Bergonié. Patients of the control cohort came from Institut Bergonié, a French sarcoma reference center. Included in the cohort were patients referred to the center for the initial diagnostic management of a soft-tissue mass of the trunk and extremities between January 2008 and January 2018 with available histological diagnosis, available pre-treatment MRI with an acceptable protocol defined as including at least one T2-WI, one pre-contrast T1-WI, one T1-WI with fat suppression after gadolinium-chelates injection (FS-Gd-T1-WI), and at least two orthogonal acquisition plans. Recurring tumors, visceral tumors, and well-differentiated liposarcomas were excluded. In total, the control cohort included 292 tumors. Of these, 10 were solitary fibrous tumors (6 malignant and 4 of intermediate malignancy), 23 were benign vascular lesions (i.e., benign vascular tumors or vascular malformations according to the International Society for the Study of Vascular Anomalies, ISSVA), 176 were non-ASPS STS (including 24 grade I, 50 grade II, and 102 grade III; details for histotypes are given in Supplementary Table 1), 33 were desmoid tumors, 18 were myxomas, and 32 were benign peripheral nerve sheath tumors (including 27 schwannomas).

The following epidemiological details were retrieved from the medical files: age, gender, histotypes, grade according to the French Federation of Cancer Centers Sarcoma Group (FNCLCC) grading system (when applicable), and location [24].

MRI acquisition

Examinations were carried out on 1.5-Tesla magnets from different radiological centers. T2-WI, T1-WI, FS-Gd-T1-WI, and at least two orthogonal acquisition plans were available for all patients. Section thickness ranged from 3 to 5 mm. Coils, field-of-view, and matrix were adapted to tumor size

and location. Ranges of repetition time/echo time were 500–700/10–15 msec for T1-WI and 2400–4500/100–130 msec for T2-WI. Different fat suppression techniques were accepted for FS-Gd-T1-WI: fat saturation, inversion-recovery imaging, opposed-phase imaging, and subtraction between post-contrast and pre-contrast T1-WI.

MRI analysis

All MRI were anonymized and double-blindedly reviewed on a Picture Archiving and Communication System (PACS) (Enterprise Imaging v8.1.2, AGFA) by two radiologists (a senior radiologist and a fellow with 2 years of experience in MRI including 6 months in a sarcoma reference center) to assess inter-observer reproducibility. A final consensus reading was made 2 months after the first readings and used for the statistical analysis.

The radiologists noted tumor depth regarding the superficial fascia and measured the longest diameter. Features depicting tumor MR signal and architecture were collected including main SI on T1-WI and T2-WI (defined as low, iso, or high, as compared to muscle), presence of a lobular architecture, presence of a fibrotic component (defined as low SI on T2-WI, low SI on T1-WI, and possible subtle enhancement on FS-Gd-T1-WI), presence of a necrotic central scar (defined as a central irregular area with variable SI on T1-WI depending on occurrence of tumor bleeding, high SI on T2-WI, no enhancement on FS-Gd-T1-WI), and presence of a fatty component (defined as high SI on T1-WI, high SI on T2-WI, low SI on FS-Gd-T1-WI). In case of doubt about SI on T1-WI and T2-WI, two regions of interest $\geq 1cm^2$ were drawn on the non-necrotic non-hemorrhagic area of the tumor and on healthy muscles; high SI was defined as $SI_{tumor}/SI_{muscle} \geq 1.1$.

Regarding tumor periphery, following features were reported: MRI growth pattern on the whole tumor circumference on T2-WI and FS-Gd-T1-WI (defined as "pushing-type" when the tumor was entirely well defined, "focal-type" and "diffuse type" when irregular borders and infiltration of surrounding tissue represented < 25% and ≥ 25% of tumor circumference, respectively [25]); presence of peritumoral edema (defined as bright SI on T2-WI beyond apparent tumor borders or pseudocapsule, without mass effect or modification of the surrounding anatomy, qualified as absent, limited, or extensive when spreading in an entire muscular compartment); presence of a peritumoral enhancement (defined as contrast enhancement within surrounding tissues, beyond apparent tumor borders or pseudocapsule, without mass effect or modification of the surrounding anatomy on FS-Gd-T1-WI); and presence of a bone invasion (defined as SI anomalies located in bone cortex and/or medulla contiguous to the tumor) or a vessel and/or nerve invasion (defined as vessel occlusion or neurovascular encasement, i.e., contact between tumor and vessel/nerve ≥ 180°) [26].

Flow-voids were defined as serpiginous or linear structures with low SI on T1-WI and T2-WI possibly in communication with feeder vessels. When flow-voids were present, the radiologists reported their distribution (defined as strictly intratumoral, strictly peritumoral, peritumoral, and intratumoral), their count (< 5 vs. ≥ 5), and their longest diameter. Peritumoral flow-void was defined as directly adjacent to the tumor, beyond the apparent tumor margins or pseudocapsule of the tumors. Intratumoral flow-void was defined as located within the tumor.

Statistical analysis

The prevalence, sensitivity, and specificity of categorical MRI features were calculated. Their association with histotype was tested using chi-square or Fisher's test as appropriate. Univariate odds ratio (OR) with 95% confidence interval (CI95%) was calculated. Continuous variables were compared using the Wilcoxon or Student test depending on the Shapiro-Wilk normality test. Inter-observer agreements were assessed using the interclass correlation coefficient with two-way mixed model (ICC) and Cohen's kappa (κ) and weighted kappa (κw) for continuous, dichotomized, and ordinal variables, respectively. The agreement for ICC was defined as good (> 0.75), moderate (0.5–0.75), or poor (< 0.5). The agreement for κ and κw was defined as slight (0–0.20), fair (0.21–0.40), moderate (0.41–0.60), substantial (0.61–0.80), and almost perfect (0.81–0.99) [27]. All tests were two-tailed. Statistical analyses were done using the SPSS statistical package (version 21.0, IBM). A p value < 0.05 was deemed significant.

Results

Population

Table 1 shows the epidemiological data of the study population. Twenty-five ASPS patients were included (16/25 women, 64%). Median age was 18.5 years old (range, 7–53). Mean age of ASPS patients was significantly lower than in the control cohort ($p < 0.0001$). Most tumors were located in the lower limb (20/25, 85%). Nineteen were intramuscular, 1 was intermuscular, and 5 were inter- and intramuscular.

Table 2 summarizes the characteristics of the cohort of patients with ASPS. The first symptom was a swelling in 19 patients, which was painful in 7 cases. The median delay from the first symptom to the histological diagnosis was 5 months (range, 1–15). Fourteen patients (14/25, 56%) had metastases at diagnosis, which were located in the lung ($n = 13$) and brain ($n = 1$). In total, 8 patients had a metastatic relapse after initial treatment, which was located in the brain ($n = 4$), bone ($n = 2$), lung ($n = 6$), and liver ($n = 1$). Five patients died of the disease, and seven are currently in complete remission.

Table 1 Clinical data of the control cohort and the cohort of patients with alveolar soft-part sarcoma

Characteristics	ASPS	Control group						
	(*n* = 25)	All (*n* = 292)	SFT (*n* = 10)	Benign vascular lesions (*n* = 23)	STS (*n* = 176)	Desmoid tumors (*n* = 33)	Myxoma (*n* = 18)	BPNST (*n* = 32)
Age	18.5 (7–53)	58 (13–92)	63.5 (35–72)	37 (16–69)	62.5 (15–92)	33 (18–76)	59.5 (36–82)	57 (16–85)
Gender								
Male	9 (36)	142 (48.6)	2 (20)	11 (47.8)	105 (59.7)	7 (21.2)	5 (27.8)	12 (37.5)
Female	16 (64)	150 (78.1)	8 (80)	12 (52.2)	71 (40.3)	26 (78.8)	13 (72.2)	20 (62.5)
Location								
Upper limb	2 (8)	34 (11.6)	1 (10)	5 (21.7)	19 (10.8)	3 (9.1)	0 (0)	6 (18.8)
Shoulder girdle	1 (4)	19 (6.5)	1 (10)	2 (8.7)	13 (7.4)	2 (6.1)	0 (0)	1 (3.1)
Trunk wall	1 (4)	55 (18.8)	3 (30)	6 (26.1)	21 (11.9)	22 (66.7)	0 (0)	3 (9.4)
Pelvic girdle	0 (0)	23 (7.9)	2 (20)	2 (8.7)	8 (4.5)	3 (9.1)	3 (16.7)	5 (15.6)
Lower limb	20 (80)	160 (54.8)	3 (30)	7 (30.4)	115 (65.3)	3 (9.1)	15 (83.3)	17 (53.1)
Other	1 (4)	1 (0.3)	0 (0)	1 (4.3)	0 (0)	0 (0)	0 (0)	2 (6.2)

Data are number of patients with percentage in parentheses, except for age given as median with range in parentheses

ASPS alveolar soft-part sarcoma, *BPNST* benign peripheral nerve sheath tumor, *SFT* solitary fibrous tumor, *STS* soft-tissue sarcoma

Associations between MRI features and ASPS

Compared to the control cohort, several MRI features were associated with ASPS (Table 3). The depth of ASPS was statistically different ($p < 0.001$), all being strictly deep-seated. Their mean size was 66 ± 30 mm, which was significantly lower than in the control cohort (80 ± 53 mm, $p = 0.045$). Main SI on T1-WI was higher than in the control group ($p < 0.001$). A fibrotic component was never seen ($p = 0.002$). MRI growth pattern of ASPS was always at least focal infiltrative, which was more frequent than for the control group ($p = 0.003$). The tail sign was never observed ($p = 0.001$). Regarding tumor vascularization, flow-voids were more numerous ($p < 0.001$) with a larger diameter ($p < 0.001$). The flow-voids distribution was statistically different ($p < 0.001$), being always intra- and peritumoral in ASPS. Only one ASPS of 30 mm did not demonstrate flow-void.

A fatty component was never seen in ASPS but it did not reach significance ($p = 0.089$). Lobular architecture was more frequently seen in ASPS without reaching significance ($p = 0.078$). When present, surrounding edema was always limited and circumscribed to lower and upper poles to the tumors. Figure 1 shows the typical aspect of ASPS on MRI with radiological-pathological correlation.

Table 4 shows the sensitivity, specificity, and odds ratio of the MRI features associated with ASPS. Strictly deep-seated location, intra- and peritumoral flow-voids, and a flow-void count ≥ 5 demonstrated sensitivity and specificity above 90%.

The MRI features demonstrated at least substantial agreements except for presence of a fibrotic component, central necrotic scar, and lobular architecture, which were moderately reproducible (Table 5).

Uniformity of ASPS presentation on MRI

All the ASPS of the series exhibited at least 5 of the 8 MRI features associated with this histotype whereas only 14% (41/292) of tumors from the control group did. Only ASPS gathered the 8 MRI features together (7/25, 28%) while none from the control group did. Twenty (20/25, 80%) ASPS demonstrated at least 7 of these 8 MRI features whereas only 4 (4/292, 1.4%) from the control group did. These 4 tumors corresponded to 2 high-grade STS (1 leiomyosarcoma and 1 undifferentiated pleomorphic sarcoma), 1 SFT, and 1 benign vascular lesion (Fig. 2). Conversely, the 5 ASPS with less than 7 of the 8 features all measured less than 40 mm. They did not exhibit necrotic central scar and flow-voids were less developed (Fig. 3).

Because ASPS may be misdiagnosed as benign vascular lesions, we conducted a sub-group analysis and compared the frequencies of each MRI feature. When compared to benign vascular lesions, ASPS from our series occurred in younger patients ($p = 0.002$). Seven MRI features were associated with ASPS: high SI on T1-WI ($p < 0.001$), no fatty component ($p = 0.002$), presence of central necrotic scar ($p = 0.001$), presence of a limited edema ($p = 0.007$), and distribution of flow-voids (benign vascular lesions having a higher proportion of strictly intratumoral vessels, $p < 0.001$) and count ($p < 0.001$). When present, the diameter of flow-void was also lower in benign vascular lesions ($p = 0.002$) (Supplementary Table 2).

Discussion

Studies about the radiological patterns of ASPS mainly consisted in case reports or small series of patients, which

Table 2 Epidemiological characteristics and outcome of the patients with alveolar soft-part sarcoma

Age, gender	First symptoms	Delay from 1st symptom to diagnosis	Location	Depth	Metastasis at diagnostic	Initial management	Outcome
7 years, male	Exophthalmos	11.5 months	Oculomotor muscle	Deep	Lung metastasis	–	Early lost to follow-up
7 years, male	Painful swelling	1 month	Shoulder girdle	Deep, intramuscular	Lung metastasis	CT, surgery, RT	Metastatic relapse 6.7 months after surgery (lung), alive 5 years later
7 years, female	Swelling	1.3 month	Thigh	Deep, intramuscular	Lung metastasis	CT, surgery, CT	No relapse, alive 33.4 months after diagnostic
11 years, female	Incidental	–	Trunk wall	Deep	Lung metastasis	CT, surgery	Lost to follow-up
12 years, male	Swelling	1.5 month	Thigh	Deep, intramuscular	No	Surgery, RT, CT	Complete remission 3 years after initial management
13 years, female	Painful swelling	4.3 months	Thigh	Deep, intramuscular	Lung metastasis	CT, surgery, RT	Metastatic relapse (lung)
15 years, male	Sport trauma	6 months	Thigh	Deep, intramuscular	No	Surgery, RT	No relapse during 3 years then lost to follow-up
16 years, male	Painful swelling	9 months	Thigh	Deep	Lung metastasis	–	–
16 years, female	Swelling	13.3 months	Thigh	Deep, intramuscular	No	Surgery	No relapse, alive R5.2 years after diagnostic
16 years, female	Painful swelling	14.8 months	Upper limb	Deep, intramuscular	No	Surgery	No relapse, alive 44.1 months after diagnostic
17 years, female	Painful swelling	3 months	Thigh	Deep, intramuscular	Lung metastasis	CT, surgery, RT	Metastatic relapse (liver and bone)
18 years, male	–	–	Upper limb	Deep, intramuscular	No	CT, surgery, RT	Metastatic relapse 42 months after surgery (lung), alive 14 years later
18 years, female	–	–	Thigh	Deep, intramuscular	Lung metastasis	CT, surgery	Lost to follow-up
19 years, female	Swelling	1.5 months	Thigh	Deep	Lung metastasis	Surgery, CT	Early lost to follow-up
22 years, female	Swelling	6 months	Thigh	Deep, intramuscular	Lung metastasis	CT, surgery	Metastatic relapse 6 months later (brain), dead of disease 22 months after initial management
23 years, female	Swelling	–	Thigh	Deep, intramuscular	Lung metastasis	–	Lost to follow-up
24 years, female	Neurologic deficit (brain metastasis)	4.3 months	Thigh	Deep, intramuscular	Brain metastasis	CT, surgery, CT	Dead of disease
28 years, female	Progressive swelling, secondarily painful	–	Thigh	Deep, intramuscular	No	Surgery	No relapse 1 year after initial management
30 years, female	Swelling	1 month	Thigh	Deep, intramuscular	No	Surgery, RT	Complete remission 5 years after initial management
31 years, female	Slowly progressive swelling	5 months	Thigh	Deep, intramuscular	No	Surgery, RT	Complete remission 3 years after initial management
32 years, female	Painful swelling	5 months	Thigh	Deep	No	CT, ILP, surgery, RT	Metastatic relapse (lung, followed by brain metastases). Died of disease 6 years after initial treatments
33 years, male	Painful swelling	12 months	Thigh	Deep, intramuscular	Lung metastasis	CT, surgery, RT	Metastatic relapse (brain and lung), died of disease
35 years, male	Swelling	–	Thigh	Deep, intramuscular	Lung metastasis	RT, surgery, CT	Stable disease since ending of adjuvant anti-angiogenic treatment
40 years, female	Swelling—mistaken for an hemangioma: arterial embolization	–	Thigh	Deep, intramuscular	No	Surgery	Local relapse 12 months after diagnosis, metastatic relapse (lung) 24 months after initial treatments
53 years, female	Swelling	1 month	Thigh	Deep, intramuscular	No	Surgery, RT	Metastatic relapse (lung, bone, brain) 12 months after initial management, died of disease 4 years later

Of the 25 patients of the series, 11 came from Institut Curie, 6 from Institut Gustave Roussy, 3 from Centre Leon Berard, 3 from Centre Oscar Lambret, and 2 from Institut Bergonié

CT chemotherapy including anti-angiogenic treatments, *ILP* isolated limb perfusion, *RT* radiotherapy

Table 3 Distribution of the MRI features according to the histotype with comparison between ASPS and control cohorts

Characteristics	ASPS	Control group							
		All	*p* value	SFT	Benign vascular lesions	STS	Desmoid tumors	Myxoma	BPNST
Longest Diameter Depth	66 ± 30	80 ± 53	0.045*	87.8 ± 41.7	55.9 ± 23.5	90 ± 56.3	87 ± 49.2	56 ± 46.1	44 ± 34.6
Superficial	0/25 (0)	12/292 (4)	< 0.001***	1/10 (10)	1/23 (4.3)	9/176 (5)	0/33 (0)	1/18 (5.6)	0/32 (0)
Deep + superficial	0/25 (0)	79/292 (27)		2/10 (20)	0/23 (0)	65/176 (37)	12/33 (36.4)	0/18 (0)	0/32 (0)
Deep, intramuscular	19/25 (76)	99/292 (34)		0/10 (0)	16/23 (69.6)	42/176 (24)	9/33 (23.7)	16/18 (88.9)	16/32 (50)
Deep, intermuscular	1/25 (4)	61/292 (21)		6/10 (60)	3/23 (13)	29/176 (16)	6/33 (18.2)	1/18 (5.6)	16/32 (50)
Deep, Inter + intramuscular	5/25 (20)	41/292 (14)		1/10 (10)	3/23 (13)	31/176 (18)	6/33 (18.2)	0/18 (0)	0/32 (0)
Main signal on T1-WI									
Hypo-	0/25 (0)	31/285 (11)	< 0.001***	0/9 (0)	2/22 (9.1)	10/173 (6)	1/32 (3)	16/17 (94.1)	2/32 (6.3)
Iso-	5/25 (20)	193/285 (68)		8/9 (88.9)	15/22 (68.2)	109/173 (63)	31/32 (97)	1/17 (5.9)	29/32 (90.6)
Hyper-	20/25 (80)	61/258 (21)		1/9 (11.1)	5/22 (22.7)	54/173 (31)	0/32 (0)	0/17 (0)	1/32 (3.1)
Main Signal on T2-WI									
Hypo-	0/23 (0)	5/291 (2)	0.637	0/10 (0)	0/23 (0)	3/175 (2)	2/33 (6)	0/18 (0)	0/32 (0)
Iso-	0/23 (0)	6/291 (2)		0/10 (0)	0/23 (0)	1/175 (1)	5/33 (15)	0/18 (0)	0/32 (0)
Hyper-	23/23 (100)	280/291 (96)		10/10 (100)	23/23 (100)	171/175 (97)	26/33 (79)	18/18 (100)	32/32 (100)
Fatty component									
No	24/24 (100)	246/276 (89)	0.089	10/10 (100)	12/19 (63.2)	141/164 (86)	33/33 (100)	18/18 (100)	32/32 (100)
Yes	0/24 (0)	30/276 (11)		0/10 (0)	7/19 (36.8)	23/164 (14)	0/33 (0)	0/18 (0)	0/32 (0)
Hemorrhagic component									
No	19/25 (76)	207/286 (72)	0.818	9/10 (90)	18/22 (81.8)	99/172 (57.6)	9/33 (27.3)	18/18 (100)	31/32 (97)
Yes	6/25 (24)	79/286 (28)		1/10 (10)	4/22 (18.2)	73/172 (42.4)	24/33 (72.7)	0/18 (0)	1/32 (3)
Fibrotic component									
No	23/23 (100)	216/292 (74)	0.002**	5/10 (50)	22/23 (95.7)	138/176 (78)	9/33 (27.3)	18/18 (100)	24/32 (75)
Yes	0/23 (0)	76/292 (26)		5/10 (50)	1/23 (4.3)	38/176 (22)	24/33 (72.7)	0/18 (0)	8/32 (25)
Central necrosis									
No	14/24 (58)	255/292 (87)	0.001**	7/10 (70)	23/23 (100)	149/176 (85)	33/33 (100)	18/18 (100)	25/32 (78.1)
Yes	10/24 (42)	37/292 (13)		3/10 (30)	0/23 (0)	27/176 (15)	0/33 (0)	0/18 (0)	7/32 (21.9)
Lobular architecture									
No	4/24 (16)	98/292 (34)	0.078	1/10 (10)	9/23 (39.1)	39/176 (22)	33/33 (100)	18/18 (100)	25/32 (78.1)
Yes	21/24 (84)	194/292 (66)		9/10 (90)	14/23 (60.9)	137/176 (78)	0/33 (0)	0/18 (0)	7/32 (21.9)
Growth pattern									
Pushing-type	0/25 (0)	94/291 (32)	0.003**	3/10 (30)	3/23 (13)	42/176 (23.9)	3/33 (9)	16/17 (94.1)	27/32 (84.4)
Focal infiltrating	15/25 (60)	113/291 (39)		6/10 (60)	11/23 (47.8)	77/176 (43.8)	14/33 (42)	1/17 (5.9)	4/32 (12.5)
Diffuse infiltrating	10/25 (40)	84/291 (29)		1/10 (10)	9/23 (39.1)	57/176 (32.4)	16/33 (49)	0/17 (0)	1/32 (3.1)
Edema									

Table 3 (continued)

Characteristics	ASPS	Control group							
		All	*p* value	SFT	Benign vascular lesions	STS	Desmoid tumors	Myxoma	BPNST
No	6/23 (26)	119/279 (41)	0.168	5/10 (50)	16/23 (69.6)	41/176 (23)	30/33 (90)	2/18 (11.1)	25/32 (78.1)
Limited	17/23 (74)	160/279 (55)		5/10 (50)	7/23 (30.4)	122/176 (69)	3/33 (10)	16/18 (88.9)	7/32 (21.9)
Extensive	0/23 (0)	13/279 (4)		0/10 (0)	0/23 (0)	13/176 (8)	0/33 (0)	0/18 (0)	0/32 (0)
Peritumoral enhancement									
No	21/23 (91)	196/287 (68)	0.068	6/10 (60)	18/23 (78.3)	92/171 (53.8)	32/33 (97)	18/18 (100)	31/32 (96.8)
Yes	2/23 (9)	91/287 (32)		4/10 (40)	5/23 (21.7)	79/171 (46.2)	1/33 (3)	0/18 (0)	1/32 (3.1)
Tail Sign									
No	25/25 (100)	207/284 (73)	0.001**	9/10 (90)	21/23 (91.3)	106/168 (63)	21/33 (64)	18/18 (100)	32/32 (100)
Yes	0/25 (0)	77/284 (27)		1/10 (10)	2/23 (8.7)	62/168 (37)	12/33 (36)	0/18 (0)	0/32 (0)
Bone, vessel, or nerves invasion									
No	18/25 (72)	220/291 (76)	0.637	6/10 (60)	22/23 (95.7)	126/176 (72)	28/33 (85)	18/18 (100)	22/32 (68.8)
Yes	7/25 (28)	71/291 (24)		4/10 (40)	1/23 (4.3)	50/176 (28)	5/33 (15)	0/18 (0)	10/32 (31.3)
Flow-voids—distribution									
None	1/25 (4)	226/292 (77)	< 0.001***	2/10 (20)	8/23 (34.8)	154/176 (87)	13/33 (39)	17/18 (94.4)	32/32 (100)
Peripheral	0/25 (0)	9/292 (3)		1/10 (10)	0/23 (0)	8/176 (5)	0/33 (0)	0/18 (0)	0/32 (0)
Internal	0/25 (0)	31/292 (11)		0/10 (0)	10/23 (43.5)	4/176 (2)	16/33 (49)	1/18 (5.6)	0/32 (0)
Peripheral + internal	24/25 (96)	26/292 (9)		7/10 (70)	5/23 (21.7)	10/176 (6)	4/33 (12)	0/18 (0)	0/32 (0)
Flow-voids—number									
< 5	2/25 (8)	265/292 (91)	< 0.001***	4/10 (40)	16/23 (69.6)	171/176 (97)	25/33 (76)	18/18 (100)	32/32 (100)
≥ 5	23/25 (92)	27/292 (9)		6/10 (60)	7/23 (30.4)	5/176 (3)	8/33 (24)	0/18 (0)	0/32 (0)
Flow-void—maximal diameter	4.6 ± 2.3	2.5 ± 1.5	< 0.001***	4.2 ± 1.7	2.5 ± 1.3	2.6 ± 1.8	4.3 ± 0.6	2	–

Data are the ratio between the numbers of patients with the MRI feature and the number of patients in who the feature was analyzable and percentage in parentheses, except for longest diameter and flow-void—maximal diameter given as mean and standard deviation

ASPS alveolar soft-part sarcoma, *BPNST* benign peripheral nerve sheath tumor, *SFT* solitary fibrous tumor; *STS*, soft-tissue sarcoma, *WI* weighted imaging. Statistical analyses consisted in chi-square tests for ordinal or categorical variables, and in Student t-test or Wilcoxon test (depending on Shapiro-Wilk normality test) for continuous variables. *$p < 0.05$, **$p < 0.005$, ***$p < 0.001$

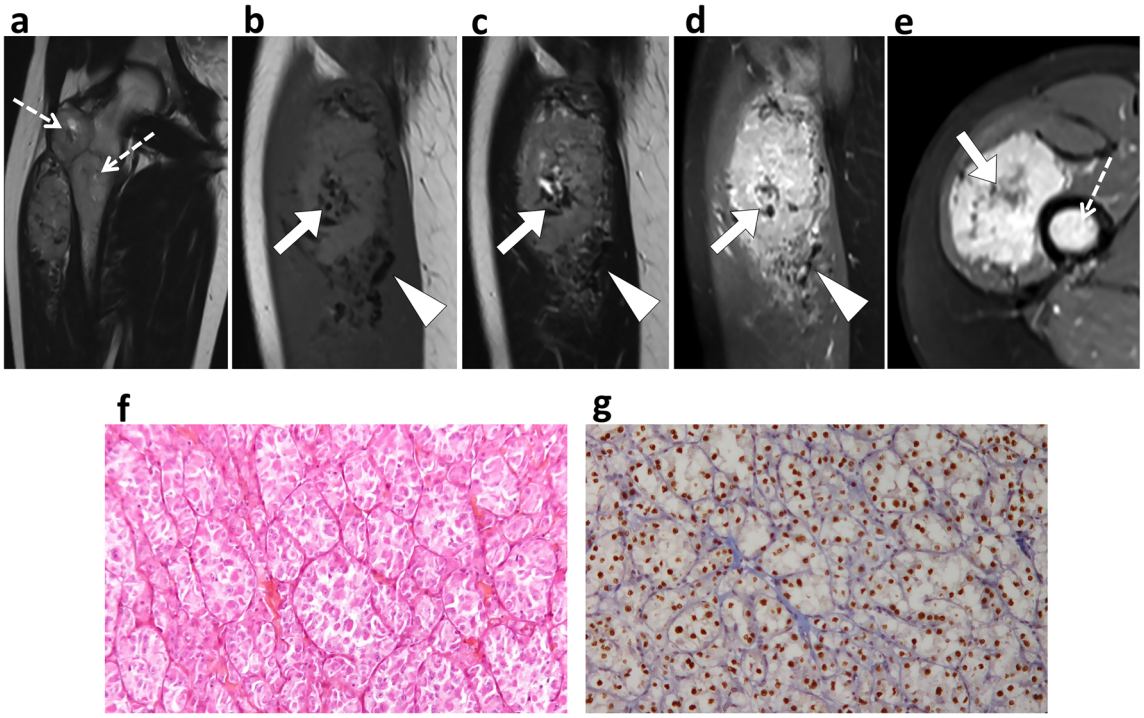

Fig. 1 Typical alveolar soft-part sarcoma—radio-pathological correlation. **a** Coronal T2-weighted imaging demonstrated a deep-seated tumor within the right quadriceps femoris with synchronous femoral bone metastases (dashed arrows). **b** On sagittal T1-weighted imaging, the tumor showed high signal intensity compared to the muscle with intra- and peritumoral abnormal vessels (white arrow and white arrowhead, respectively) at its upper and lower poles with low signal intensity, also on sagittal T2-weighted imaging (**c**) and on sagittal fat-sat T1-weighted imaging after Gadolinium-chelates injection (**d**). Axial fat saturated T1-weighted imaging after Gadolinium-chelates injection (**e**) shows a central area without enhancement corresponding to the necrotic central scar (white arrow) and one of the bone metastases (dashed arrow). **f** Hematoxylin and Eosin stained slices shows the typical pseudoalveolar organization of large eosinophilic cells separated by fibrovascular thin septa with abundant capillaries. **g** Immunohistochemistry showing nuclear positivity for TFE3 due to the abnormal expression of the ASPL-TFE3 fusion protein

enabled the identification of recurrent imaging features and differential diagnoses among pseudo-tumors and benign or malignant soft-tissue tumors. We report herein the largest series of ASPS with their initial MRI, all with a contrast-agent administration prior to treatment. Furthermore, we systematically compared the distribution of classical radiological features of ASPS with those of a control cohort to test their diagnostic value. Altogether, our results identified 8 features associated with ASPS: a strictly deep situation, high SI on T1-WI, an area of central necrosis, the absence of fibrotic component, an infiltrative growth pattern, the presence of intra- and peritumoral flow-voids, with more than 5 flow-voids, and the absence of tail sign. All the large ASPS (> 40 mm) shared at least 7 of these 8 radiological characteristics, illustrating the uniformity of their phenotype. On the contrary, smaller ASPS may not demonstrate central necrosis or flow-voids, thus running the risk of

Table 4 Sensitivity, specificity, and odds ratio of the MRI features associated with alveolar soft-part sarcoma

Characteristics	Sensitivity	Specificity	OR	*p* value
Strictly deep-seated	100 (86.7–100)	90.8 (86.9–93.6)	+∞ (–;–)	< 0.001
High main SI on T1-WI	80 (60.9–91.1)	78.6 (73.5–83)	14.7 (5.3–40.7)	< 0.001
No fibrotic area	100 (85.7–100)	26 (21.3–31.4)	+∞ (–;–)	0.005
Area of central necrosis	41.7 (24.5–61.2)	87.3 (83–90.7)	4.9 (2.0–11.9)	0.001
Focal or diffuse infiltrative growth pattern	100 (86.7–100)	32 (27.2–37.9)	+∞ (–;–)	0.001
No tail sign	100 (86.7–100)	27.1 (22.3–32.6)	+∞ (–;–)	0.004
Intra and peripheral flow-voids	96 (80.5–99.3)	91.1 (87.3–93.9)	245 (32–1889)	< 0.001
Flow-void number ≥ 5	92 (75–97.8)	90.8 (86.7–93.6)	112.9 (25–505)	< 0.001

Sensitivity, specificity, and odds ratio are given as percentages with 95% confidence intervals. *OR* odds ratio, *SI* signal intensity, *WI* weighted-imaging. The *p* value corresponds to the *p* value of the Fisher's test (after dichotomization in case of ordinal or categorical variables with more than two outcomes)

Table 5 Inter-observer agreement of the MRI features

Characteristics	Inter-observer agreement
Longest diameter[a]	0.979 (0.972–0.983)
Depth[b]	0.844 (0.770–0.918)
Main signal on T1-WI[c]	0.620 (0.528–0.712)
Main signal on T2-WI[c]	0.864 (0.819–0.909)
Fatty component[b]	0.651 (0.498–0.804)
Hemorrhagic component[b]	0.694 (0.594–0.794)
Fibrotic component[b]	0.465 (0.308–0.622)
Necrotic central scar[b]	0.468 (0.319–0.617)
Lobular architecture[b]	0.541 (0.421–0.661)
Growth pattern[c]	0.666 (0.566–0.766)
Peritumoral edema[c]	0.665 (0.600–0.730)
Peritumoral enhancement[b]	0.600 (0.494–0.706)
Tail sign[b]	0.697 (0.589–0.805)
Bone, vessel, or nerve invasion[b]	0.710 (0.604–0.816)
Flow-void—distribution[b]	0.631 (0.529–0.733)
Flow-void—maximal diameter[a]	0.801 (0.751–0.843)
Flow-void—number[c]	0.850 (0.764–0.936)

The following statistical tests were used: [a] ICC, [b] kappa, and [c] weighted kappa. *WI* weighted imaging

being confused with benign tumors. Moreover, age can be a helpful factor to take into account in the differential diagnosis as most ASPS occur in adolescent and young adult.

The clinical and radiological findings of our series are in agreement with previously reported features of ASPS. Most tumors presented with deep-seated masses. Median age was 18.5 years old, while it ranged from 15.5 to 36 years old in other series. Patients were predominantly women. None of the previous radiological studies found superficial ASPS. Interestingly, a myogenic differentiation has been hypothesized for ASPS, which may explain this recurrent deep intramuscular situation [28–31]. More than half of the patients of our series had metastasis at diagnosis, which is more than usual (20–30%) although Li et al found similar statistics [10, 14, 15, 32, 33]. In our series, 20% of patients presented with brain metastases at diagnosis or during follow-up, which is uncommon for sarcomas and questions systematic brain CT scan or MRI for follow-up. Metastatic onset is a major prognostic factor for ASPS [14].

Almost all ASPS of our series had an abnormal vasculature in keeping with the translocation-induced angiogenesis displayed by these tumors [34–36]. ASPS had a higher number of flow-voids of a longer diameter as compared to other soft-tissue tumors, with both intra- and peritumoral vessels. Flow-voids were also seen in several SFT, benign vascular lesions, some STS, and desmoid tumors. None were noticed in BPNST and myxoma except for one patient although Kato and al reported cases of BPNST with flow-voids [18]. In comparison, McCarville and colleagues found flow-voids in all ASPS, which were mostly located in the upper and lower poles when peritumoral. They reported the occurrence of thrombosis of these large vessels; however, we did not observe this event [11].

Regarding their periphery, ASPS from our series all demonstrated at least a focal-type infiltrative growth pattern, but they never exhibited aponeurotic spreading. Previous studies also stressed the ill-defined margins, micro-infiltrative margins of ASPS, without capsule. Lobulated contours were also frequently observed, in agreement with McCarville et al, but this feature was not discriminant when compared to the control cohort and to the benign vascular tumors in our study [11].

From a practical point of view, all patients with an undetermined deep soft-tissue mass should undergo ultrasounds and MRI and be referred to a sarcoma reference center for biopsy and appropriate management [37]. Nonetheless, we identified a risk of confusion between benign intramuscular vascular lesions and ASPS. Both histotypes can occur in young patients and are mostly deep-seated in the lower limb with possible small flow-voids, lobular architecture, irregular borders, and lack of central area of necrosis. Hence, when faced with a possible small intramuscular benign vascular tumor or vascular malformation, recommending a simple clinical and radiological follow-up instead of a biopsy may be risky. To avoid this, it could be useful look for a fatty component, which was never seen in ASPS but in 63.2% of intramuscular hemangioma and ask for a computed tomography to investigate the presence of calcification or phleboliths, which are common in intramuscular hemangioma [38]. It should be noted that these studies regarding intramuscular hemangioma used the WHO classification of soft-tissue tumors instead of the ISSVA classification, which is at risk of confusion with intramuscular benign vascular tumors or intramuscular vascular malformations [1, 39]. Moreover, the systematic biopsy of suspected intramuscular benign vascular tumor or vascular malformation could be questioned.

SFT of extremities and trunk wall could also be mistaken for ASPS, as they can present with intra and peritumoral vessels, lobular architecture, irregular margins, iso- to high SI on T1-WI, necrosis, and deep situation [21, 40, 41]. To help discriminating SFT from ASPS, it should be noted that SFT classically shows variables SI on T2-WI with a "black-and-white-mixed" pattern [42] and are rarely intramuscular. Conversely, a fibrous component was never seen in ASPS from our series and never reported in any radiological series about ASPS.

Two STS (one undifferentiated pleomorphic sarcoma and one leiomyosarcoma) shared all the MRI features associated with ASPS, but they occurred in older patients (> 60 years old here). Twenty-two patients with STS demonstrated flow-voids. Most were high-grade STS and the associations between occurrence of an abnormal vasculature, overexpression of pro-angiogenic factors, and occurrence of metastasis in non-ASPS STS could be questioned.

We decided to maintain the distinction between intra- and peritumoral flow-voids among the MRI criteria in order to describe as exhaustively as rationally possible the tumors of

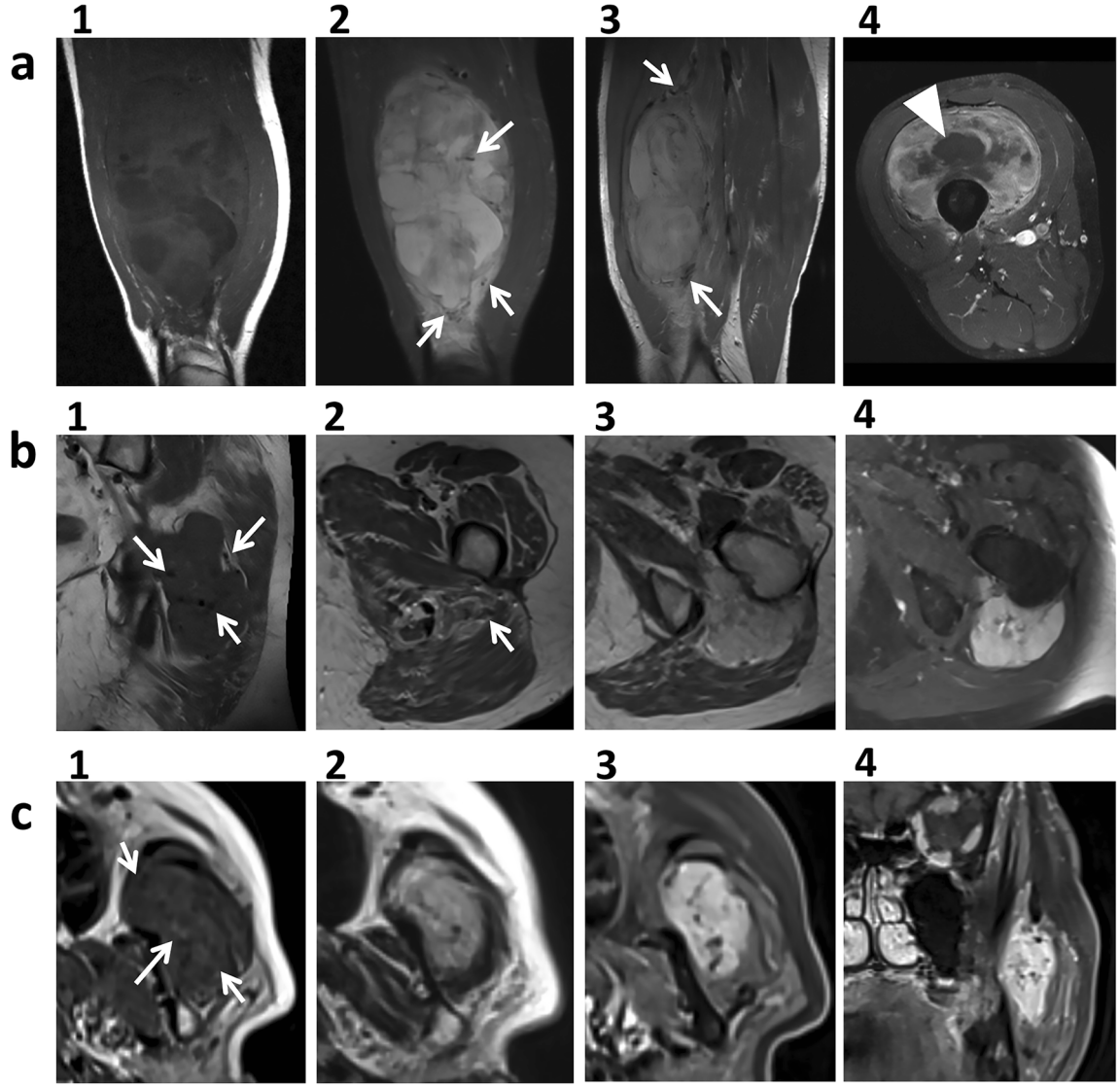

Fig. 2 Soft-tissue tumors sharing the MRI features associated with alveolar soft-part sarcoma. These tumors all demonstrated a deep location, focal infiltrative growth pattern without tail sign, high SI on T1-weighted imaging, more than 5 intra- and peritumoral flow-voids (white arrows), and no fibrotic area, with eventual necrotic central scar (white arrow heads). **a** Deep-seated undifferentiated pleomorphic sarcoma of the quadriceps femoris. (1: coronal T1-weighted imaging, 2: coronal STIR T2-weighted imaging, 3: sagittal T2-weighted imaging, and 4: axial fat-sat T1-weighted imaging after gadolinium-chelates injection). **b** Deep-seated solitary fibrous tumor of the left ischio-femoral space (1: coronal T1-weighted imaging, 2: axial T2-weighted imaging at the lower pole of the tumor, 3: axial T2-weighted imaging, and 4: axial fat-sat T1-weighted imaging after gadolinium-chelates injection). **c** Deep-seated intramuscular hemangioma of the left masseter muscle (1: axial T1-weigted imaging, 2: axial T2-weighted imaging, 3: axial, and 4: coronal fat-sat T1-weighted imaging after gadolinium-chelates injection)

our series. These findings have been frequently reported in previous studies regarding ASPS, but their diagnostic value was not investigated. The distinction between intra- and peritumoral flow-voids in several histotypes provided original insights regarding the vascularization of soft-tissue tumors. In our series, flow-voids in ASPS, desmoid tumors, or benign vascular lesions were never strictly peritumoral. Only STS and SFT showed strictly peripheral flow-voids. In the same way, strictly intratumoral flow-voids were only seen in benign vascular lesions, STS, desmoid tumors, and in one myxoma.

This retrospective series is limited by the heterogeneity of MRI protocols as MRI data were secondarily referred to our tertiary care reference center. Fat suppression was not mandatory for T1-WI sequences; some MRI did not include pre-contrast fat-suppressed T1-WI. Furthermore, the fat suppression technique for FS-Gd-T1-WI sequences was not standardized, which may have complicated the signal interpretation of fatty component. The fatty component was identified as high SI on T1-WI, high SI on T2-WI, and no enhancement on FS-Gd-T1-WI. Consequently, we applied a simple qualitative or semi-quantitative analysis grid. None of the ASPS demonstrated a fibrotic component on MRI, which was defined as low SI on T2-WI and T1-WI; however, it should be noted that calcification and hemosiderin can also demonstrate these findings on MRI.

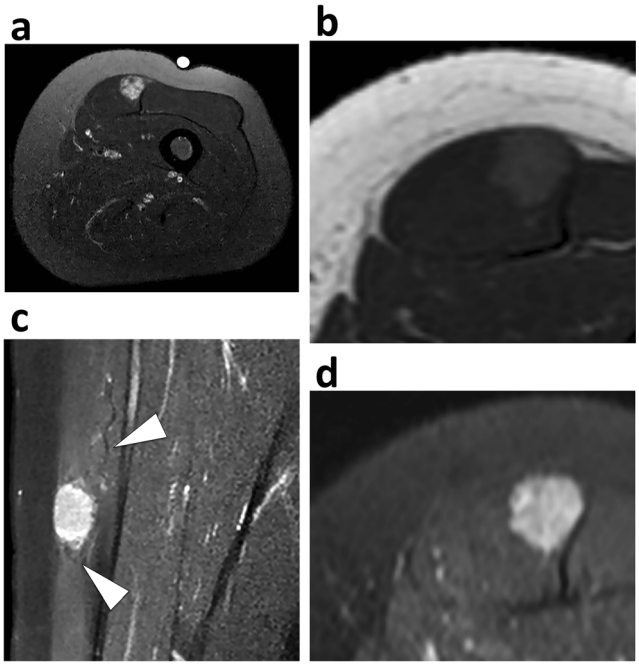

Fig. 3 Small alveolar soft-part sarcoma. **a** Axial STIR T2-weighted imaging showed a 2-cm large deep-seated tumor of the right quadriceps femori with heterogeneous high signal intensity on T2-weighted imaging. On axial T1-weighted imaging (**b**), the tumor demonstrated high signal intensity. On coronal (**c**) and axial fat-sat (**d**) T1-weighted imaging after gadolinium-chelates injection, small and thin vessels (white arrow heads) were seen around the tumor. The margins of the tumors are irregular with focal infiltrative growth pattern

Quantitative imaging features extracted from diffusion-weighted imaging or dynamic contrast-enhanced MRI may have helped to improve characterization of ASPS, but they were almost never performed. Moreover, our study is a case-control study. If this design is well adapted for rare disease, such as ASPS, this is at risk of selection bias. The proportions of tumors demonstrating the MRI features in the ASPS cohort and the control cohort may not perfectly represent the proportions in the general population. To limit the selection bias, we built the largest possible cohort of ASPS patients with an available initial contrast-enhanced MRI from five large comprehensive cancer centers of our country. In addition, we built a control cohort of soft-tissue masses of extremities and trunk walls with available contrast-enhanced MRI, based on the 10-year long activity (i.e., since the installation of a PACS) of one of the three French sarcoma reference centers. With 292 MRIs, this control cohort is here again one of the largest, even if some histotypes were not represented. Indeed, we excluded well-differentiated liposarcoma for which the real diagnostic challenge is the distinction from lipoma. Our control cohort did not include neither the imaging of angiosarcoma or dermatofibrosarcoma (as the patients mostly presented with superficial lesions which rarely require an MRI) nor the imaging of some benign histotypes [43, 44]. Actually, most of these benign histotypes do not share the MRI features reported in ASPS; hence, we believe that their inclusion in the control cohort would have rather led to increasing the sensitivity and specificity of the MRI features associated with ASPS. On the other hand, we included all the most common histotypes of soft-tissue tumors and histotypes that were quoted as potential differential diagnosis of ASPS. Systematic radiological-histopathological correlations were not performed to confirm the MRI findings, notably regarding the tumor vascularization. However, all the histological diagnoses were confirmed by expert pathologists from sarcoma reference centers.

Finally, it should be kept in mind that a soft-tissue mass with abnormal vasculature and contrast uptake may be a metastasis of a hypervascular tumor such as renal cell or thyroid carcinoma.

To conclude, our study put in perspective the MRI features of a large series of ASPS with those of a control cohort that included several of their differential diagnoses. Age should also be carefully considered when establishing the diagnostic hypotheses of a vascularized soft-tissue mass. Even if these defining MRI features are specific, small ASPS may be misdiagnosed.

Acknowledgements The authors would like to thank Ms. Camille Martinerie for medical writing services.

Funding The authors state that this work has not received any funding.

Compliance with ethical standards

Guarantor The scientific guarantor of this publication is Dr. Michèle Kind, MD, MSc, Department of Radiology, Institut Bergonié, Bordeaux, France.

Conflict of interest The authors of this manuscript declare no relationships with any companies, whose products or services may be related to the subject matter of the article.

Statistics and biometry No complex statistical methods were necessary for this paper.

Informed consent Written informed consent was waived by the Institutional Review Board.

Ethical approval Institutional Review Board approval was obtained.

Study subjects or cohorts overlap Six patients were previously reported in the study by Viry et al, which was a series of cases without extensive radiological analysis and without comparison to other potential differential diagnoses (Pediatr Radiol. 2013;43(9):1174–81).

Methodology
- Retrospective
- Case/control study
- Multicenter study

References

1. Fletcher CDM, Bridge JA, Hogendoorn P, Mertens F (2013) WHO classification of tumours of soft tissue and bone, 4th edn. IARC Press, Lyon

2. Ferrari A, Sultan I, Huang TT et al (2011) Soft tissue sarcoma across the age spectrum: a population-based study from the surveillance epidemiology and end results database. Pediatr Blood Cancer 57: 943–949. https://doi.org/10.1002/pbc.23252
3. Christopherson WM, Foote FW Jr, Stewart FW (1952) Alveolar soft-part sarcomas; structurally characteristic tumors of uncertain histogenesis. Cancer 5:100–111
4. Ladanyi M, Lui MY, Antonescu CR et al (2001) The der(17)t(X;17)(p11;q25) of human alveolar soft part sarcoma fuses the TFE3 transcription factor gene to ASPL, a novel gene at 17q25. Oncogene 20:48–57. https://doi.org/10.1038/sj.onc.1204074
5. Viry F, Orbach D, Klijanienko J et al (2013) Alveolar soft part sarcoma-radiologic patterns in children and adolescents. Pediatr Radiol 43:1174–1181. https://doi.org/10.1007/s00247-013-2667-4
6. Cui JF, Chen HS, Hao DP, Liu JH, Hou F, Xu WJl (2017) Magnetic resonance features and characteristic vascular pattern of alveolar soft-part sarcoma. Oncol Res Treat 40:580–585. https://doi.org/10.1159/000477443
7. Itani M, Shabb NS, Haidar R, Khoury NJ (2013) AIRP best cases in radiologic-pathologic correlation: alveolar soft-part sarcoma. Radiographics 33:585–593. https://doi.org/10.1148/rg.332115173
8. Iwamoto Y, Morimoto N, Chuman H, Shinohara N, Sugioka Y (1995) The role of MR imaging in the diagnosis of alveolar soft part sarcoma: a report of 10 cases. Skeletal Radiol 24:267–270
9. Kim HS, Lee HK, Weon YC, Kim HJ (2005) Alveolar soft-part sarcoma of the head and neck: clinical and imaging features in five cases. AJNR Am J Neuroradiol 26:1331–1335
10. Li X, Ye Z (2014) Magnetic resonance imaging features of alveolar soft part sarcoma: report of 14 cases. World J Surg Oncol 12:36. https://doi.org/10.1186/1477-7819-12-36
11. McCarville MB, Muzzafar S, Kao SC et al (2014) Imaging features of alveolar soft-part sarcoma: a report from children's oncology group study ARST0332. AJR Am J Roentgenol 203:1345–1352. https://doi.org/10.2214/AJR.14.12462
12. Sood S, Baheti AD, Shinagare AB et al (2014) Imaging features of primary and metastatic alveolar soft part sarcoma: single institute experience in 25 patients. Br J Radiol 87:20130719. https://doi.org/10.1259/bjr.20130719
13. Suh JS, Cho J, Lee SH et al (2000) Alveolar soft part sarcoma: MR and angiographic findings. Skeletal Radiol 29:680–689
14. Portera CA Jr, Ho V, Patel SR et al (2001) Alveolar soft part sarcoma: clinical course and patterns of metastasis in 70 patients treated at a single institution. Cancer 91:585–591
15. Lieberman PH, Brennan MF, Kimmel M, Erlandson RA, Garin-Chesa P, Flehinger BY (1989) Alveolar soft-part sarcoma. A clinico-pathologic study of half a century. Cancer 63:1–13
16. Setsu N, Yoshida A, Takahashi F, Chuman H, Kushima R (2014) Histological analysis suggests an invasion-independent metastatic mechanism in alveolar soft part sarcoma. Hum Pathol 45:137–142. https://doi.org/10.1016/j.humpath.2013.07.045
17. Ordóñez NG, Mackay B (1998) Alveolar soft-part sarcoma: a review of the pathology and histogenesis. Ultrastruct Pathol 22:275–292
18. Kato H, Kanematsu M, Mizuta K et al (2010) "Flow-void" sign at MR imaging: a rare finding of extracranial head and neck schwannomas. J Magn Reson Imaging 31:703–705. https://doi.org/10.1002/jmri.22071
19. Kim JY, Lee JH, Nam JG, Choi SH, Seo YW, Jeong YK (2014) Value of tumor vessel sign in isolated circumscribed hypervascular abdominopelvic mesenchymal tumors on multidetector computed tomography. J Comput Assist Tomogr 38:747–752. https://doi.org/10.1097/RCT.0000000000000099
20. Robbin MR, Murphey MD, Temple HT, Kransdorf MJ, Choi JJ (2001) Imaging of musculoskeletal fibromatosis. Radiographics 21: 585–600. https://doi.org/10.1148/radiographics.21.3.g01ma21585
21. Ginat DT, Bokhari A, Bhatt S, Dogra V (2011) Imaging features of solitary fibrous tumors. AJR Am J Roentgenol 196:487–495. https://doi.org/10.2214/AJR.10.4948
22. Musyoki FN, Nahal A, Powell TI (2012) Solitary fibrous tumor: an update on the spectrum of extrapleural manifestations. Skeletal Radiol 41:5–13. https://doi.org/10.1007/s00256-010-1032-z
23. Conticabase - European sarcoma database and tumour bank (n.d.) https://conticabase.sarcomabcb.org/
24. Trojani M, Contesso G, Coindre JM et al (1984) Soft-tissue sarcomas of adults; study of pathological prognostic variables and definition of a histopathological grading system. Int J Cancer 33:37–42
25. Nakamura T, Matsumine A, Matsubara T et al (2017) Infiltrative tumor growth patterns on magnetic resonance imaging associated with systemic inflammation and oncological outcome in patients with high-grade soft-tissue sarcoma. PLoS One 12:e0181787. https://doi.org/10.1371/journal.pone.0181787
26. Holzapfel K, Regler J, Baum T et al (2015) Local staging of soft-tissue sarcoma: emphasis on assessment of neurovascular encasement-value of MR imaging in 174 confirmed cases. Radiology 275(2):501–509. https://doi.org/10.1148/radiol.14140510
27. Landis JR, Koch GG (1977) The measurement of observer agreement for categorical data. Biometrics 33:159–174. https://doi.org/10.2307/2529310
28. Rosai J, Dias P, Parham DM, Shapiro DN, Houghton P (1991) MyoD1 protein expression in alveolar soft part sarcoma as confirmatory evidence of its skeletal muscle nature. Am J Surg Pathol 15:974–981
29. Tallini G, Parham DM, Dias P, Cordon-Cardo C, Houghton PJ, Rosai J (1994) Myogenic regulatory protein expression in adult soft tissue sarcomas. A sensitive and specific marker of skeletal muscle differentiation. Am J Pathol 144:693–701
30. Stockwin LH, Vistica DT, Kenney S et al (2009) Gene expression profiling of alveolar soft-part sarcoma (ASPS). BMC Cancer 9:22. https://doi.org/10.1186/1471-2407-9-22
31. Folpe AL, Deyrup AT (2006) Alveolar soft-part sarcoma: a review and update. J Clin Pathol 59:1127–1132. https://doi.org/10.1136/jcp.2005.031120
32. Lazar AJ, Das P, Tuvin D et al (2007) Angiogenesis-promoting gene patterns in alveolar soft part sarcoma. Clin Cancer Res 13: 7314–7321. https://doi.org/10.1158/1078-0432.CCR-07-0174
33. Pennacchioli E, Fiore M, Collini P et al (2010) Alveolar soft part sarcoma: clinical presentation, treatment, and outcome in a series of 33 patients at a single institution. Ann Surg Oncol 17:3229–3233. https://doi.org/10.1245/s10434-010-1186-x
34. Kummar S, Allen D, Monks A et al (2013) Cediranib for metastatic alveolar soft part sarcoma. J Clin Oncol 31:2296–2302. https://doi.org/10.1200/JCO.2012.47.4288
35. Stacchiotti S, Negri T, Zaffaroni N et al (2011) Sunitinib in advanced alveolar soft part sarcoma: evidence of a direct antitumor effect. Ann Oncol 22:1682–1690. https://doi.org/10.1093/annonc/mdq644
36. Schöffski P, Wozniak A, Kasper B et al (2018) Activity and safety of crizotinib in patients with alveolar soft part sarcoma with rearrangement of TFE3: European Organization for Research and Treatment of Cancer (EORTC) phase II trial 90101 "CREATE". Ann Oncol 29:758–765. https://doi.org/10.1093/annonc/mdx774
37. Noebauer-Huhmann IM, Weber MA, Lalam RK et al (2015) Soft tissue tumors in adults: ESSR-approved guidelines for diagnostic imaging. Semin Musculoskelet Radiol 19:e1. https://doi.org/10.1055/s-0036-1572350
38. Griffin N, Khan N, Thomas JM, Fisher C, Moskovic EC (2007) The radiological manifestations of intramuscular haemangiomas in adults: magnetic resonance imaging, computed tomography and ultrasound appearances. Skeletal Radiol 36:1051–1059. https://doi.org/10.1007/s00256-007-0375-6
39. Wassef M, Blei F, Adams D et al (2015) Vascular anomalies classification: recommendations from the International Society for the

Study of Vascular Anomalies. Pediatrics 136(1):e203–e214. https://doi.org/10.1542/peds.2014-3673

40. Wignall OJ, Moskovic EC, Thway K, Thomas JM (2010) Solitary fibrous tumors of the soft tissues: review of the imaging and clinical features with histopathologic correlation. AJR Am J Roentgenol 195:W55–W62. https://doi.org/10.2214/AJR.09.3379
41. Garcia-Bennett J, Olivé CS, Rivas A, Domínguez-Oronoz R, Huguet P (2012) Soft tissue solitary fibrous tumor. Imaging findings in a series of nine cases. Skeletal Radiol 41:1427–1433. https://doi.org/10.1007/s00256-012-1364-y
42. Weon YC, Kim EY, Kim HJ, Byun HS, Park K, Kim JH (2007) Intracranial solitary fibrous tumors: imaging findings in 6 consecutive patients. AJNR Am J Neuroradiol 28:1466–1469. https://doi.org/10.3174/ajnr.A0609
43. Kransdorf MJ (1995) Malignant soft-tissue tumors in a large referral population: distribution of diagnoses by age, sex, and location. AJR Am J Roentgenol 164:129–134. https://doi.org/10.2214/ajr.164.1.7998525
44. Kransdorf MJ (1995) Benign soft-tissue tumors in a large referral population: distribution of specific diagnoses by age, sex, and location. AJR Am J Roentgenol 164:395–402. https://doi.org/10.2214/ajr.164.2.7839977